3D printing, Bioprinting and Medical Data Processing

Zbigniew Starosolski, Ph.D.
Associate Professor
Translational Imaging Group: TIGr
Department of Radiology

Rice Biomedical Tech Forum 10/28/2024

Texas Children's®

BCM Baylor College of Medicine

Agenda

- 3D printing for hospital needs
  - anatomical models
  - swabs
- Bio-printing
  - Mic-MPS
- ML and Radiomics research
  - TAM micro-environment
  - Aortic dissection
- Clinical Diagnostics
  - Lung inflammation
- Clinical prognostication
  - Not Accidental Trauma

3D Printing for Hospital Needs

Texas Children's®

BCM
Baylor College of Medicine

Surgery planning

A 10-year-old female.
(a) Radiograph, (b) 3-D rendering and (c) 3-D print from CT data show healing Herring class 3 Perthes disease. (d, e) Three-dimensional prints can be used to simulate proposed surgical corrections. (f) Radiograph after subtrochanteric valgus osteotomy of the right femur to align the more medially located spherical component of the femoral head to the weight-bearing portion of the hip joint

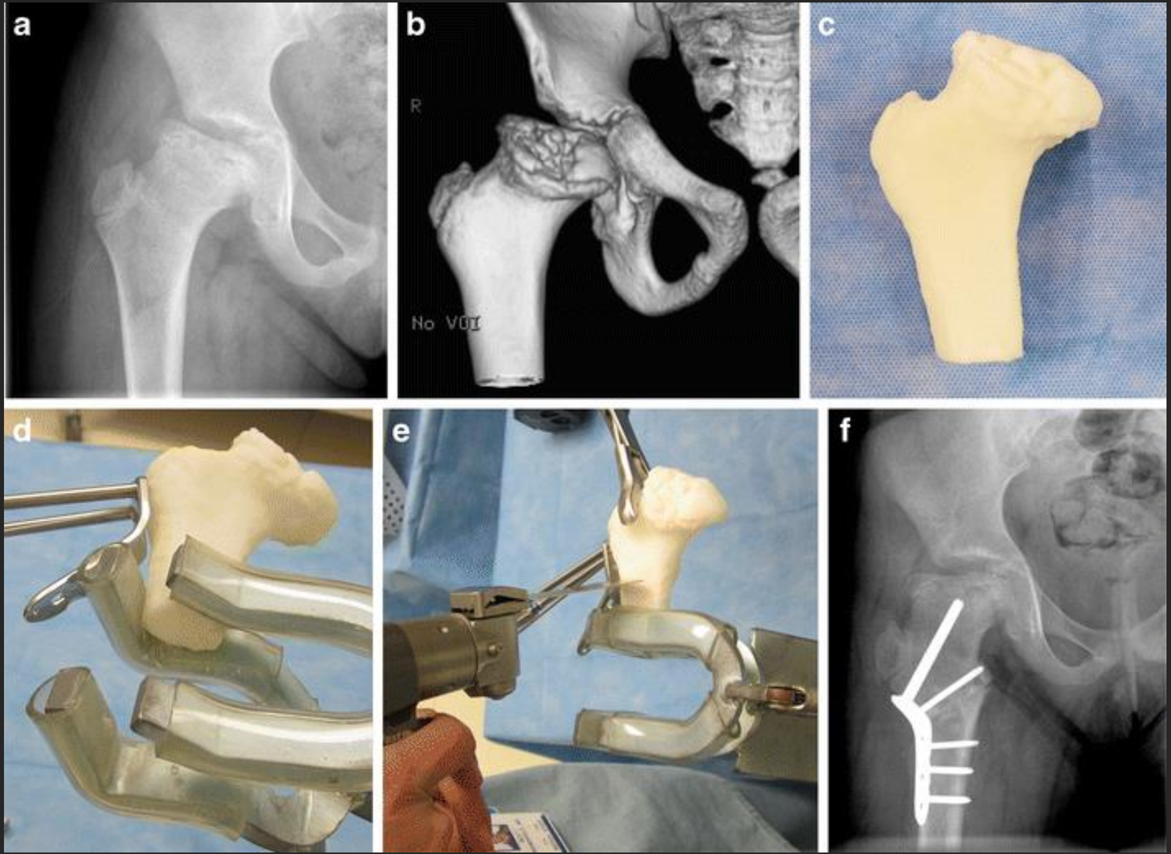

Starosolski Z.A. et al. Application of 3-D printing (rapid prototyping) for creating physical models of pediatric orthopedic disorders. Pediatr Radiol. 2014

Major Aorto-Pulmonary Collateral Arteries

- develop early in embryonic life
- do not regress as the pulmonary artery develop
- continue to grow
- pulmonary hypertension
- oxygen deficient
- excess of CO2
- acidosis

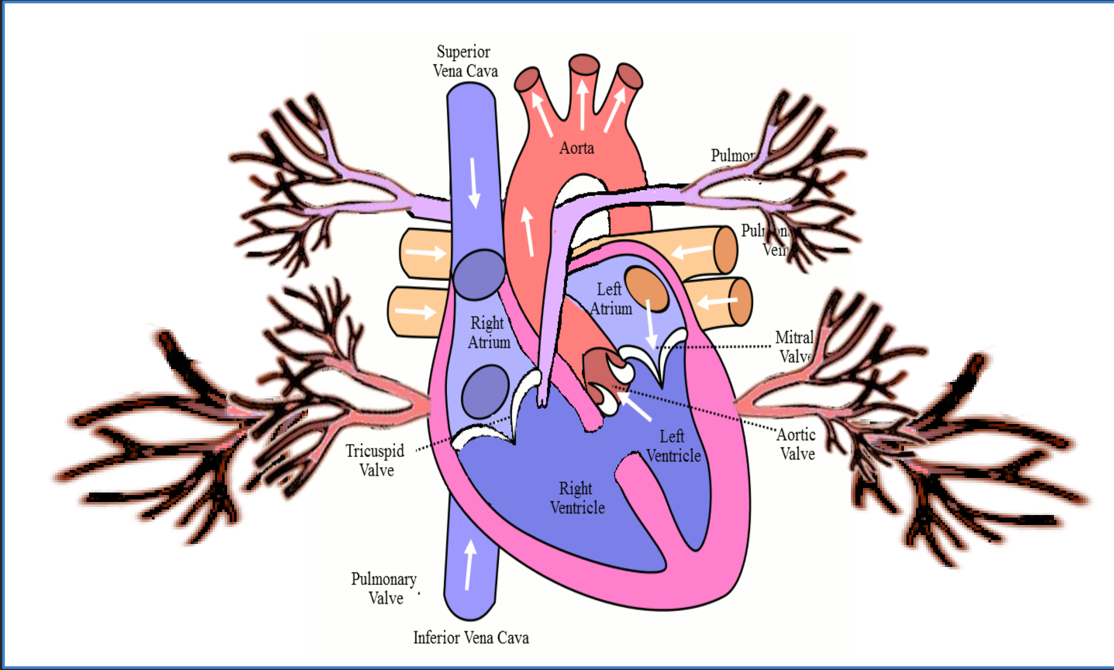

Major Aorto-Pulmonary Collateral Arteries

Fig. FDM 3D printed anatomical model using POLO-LAY Lay-Form filament and PVA water soluble supporting material

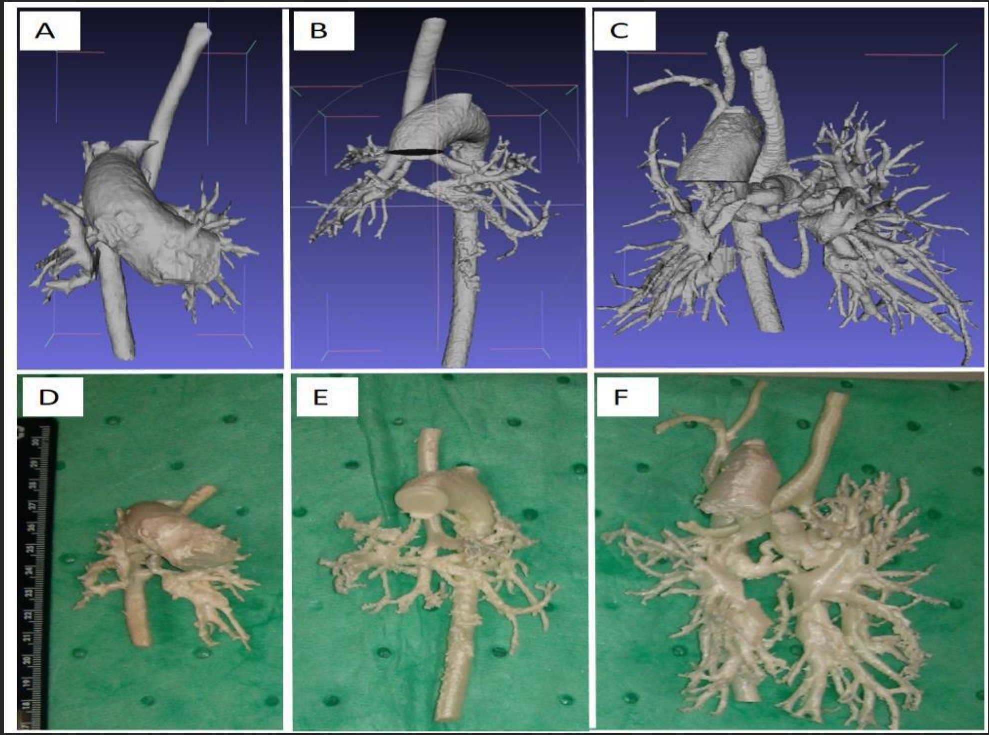

Fig. A-C 3D surface models of MAPCAs, D-F 3D printed anatomical flexible models

Major Aorto-Pulmonary Collateral Arteries

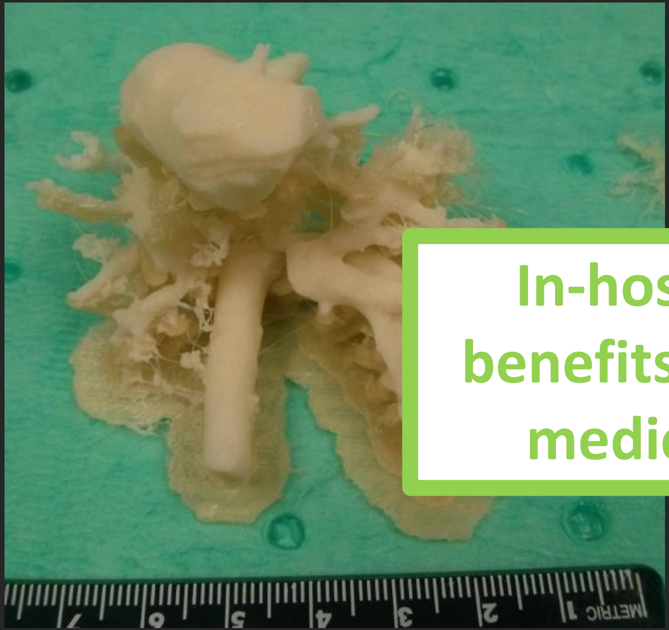

Fig. FDM 3D printed anatomical model using POLO-LAY Lay-Form filament and PVA water soluble supporting material

In-hospital 3D printing benefits both patients and medical professionals

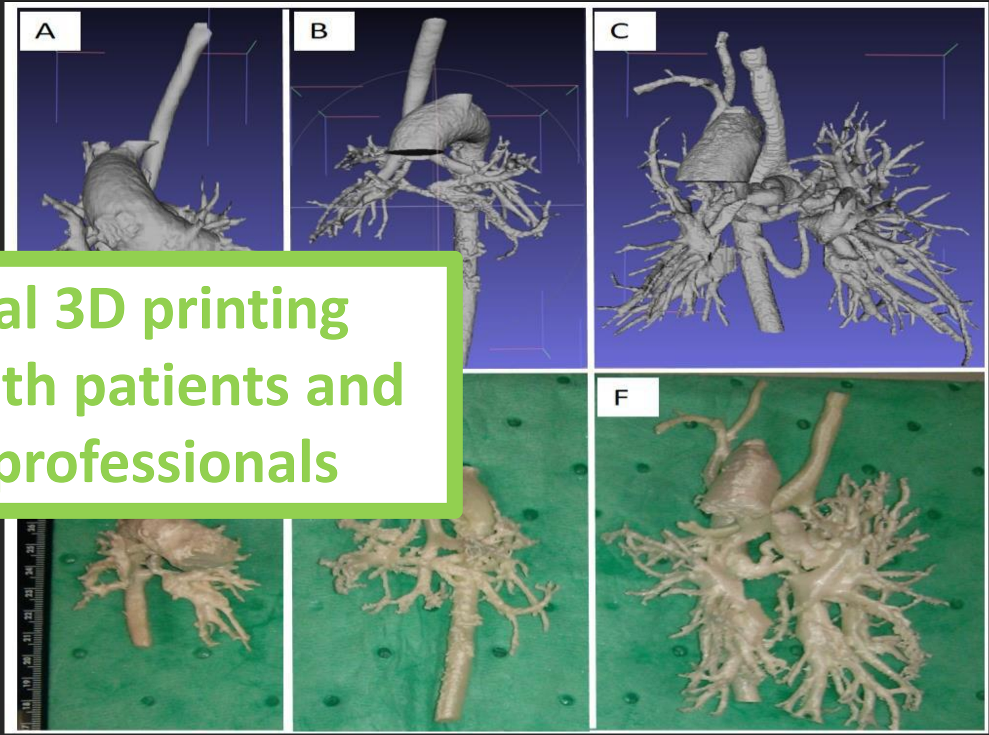

Fig. A-C 3D surface models of MAPCAs, D-F 3D printed anatomical flexible models

USF Health 3D-printed nasal swab used in pandemic

- Solution to the disrupted commercial production of standard flocked NP
- Comparable to conventional nasopharyngeal swabs
- obtain enough viral particles -> reliable diagnosis of COVID-19
- The FDA has given clearance for the use of 3D printed swabs that use medical/dental grade materials
- Institutions with access to approved printers and material can produce and use these swabs for testing
- Class I devices exempt from premarket notifications according to 21 CFR § 880.6025 Absorbent tipped applicator

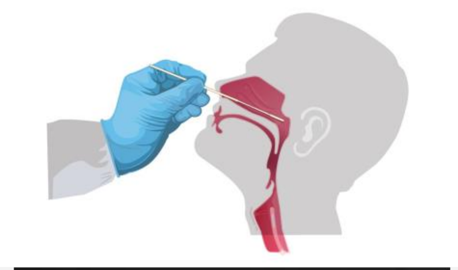

Surgial Guide Resin is non-cytotoxic, not a sensitizer, non-irriating, and complies with ISO 109933-1:2018.

https://www.cdc.gov/covid/hcp/clinical-care/clinical-specimen-guidelines.html

From Bench to Clinic: Pediatric Swabs

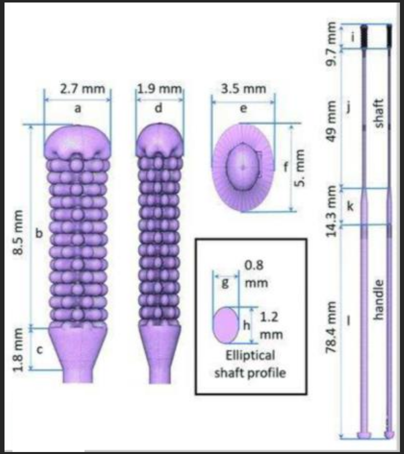

CT scan → CAD design candidates → Testing and sellection → Manufacturing for hospital internal needs

Starosolski Z, Admane P, Dunn J, Kaziny B, Huisman TAGM, Annapragada A. Design of 3D-Printed Nasopharyngeal Swabs for Children is Enabled by Radiologic Imaging. AJNR Am J Neuroradiol. 2020 Dec;41(12):2345-2347. doi: 10.3174/ajnr.A6794. Epub 2020 Aug 27. PMID: 32855191; PMCID: PMC7963225.

3D printed elastic models testing

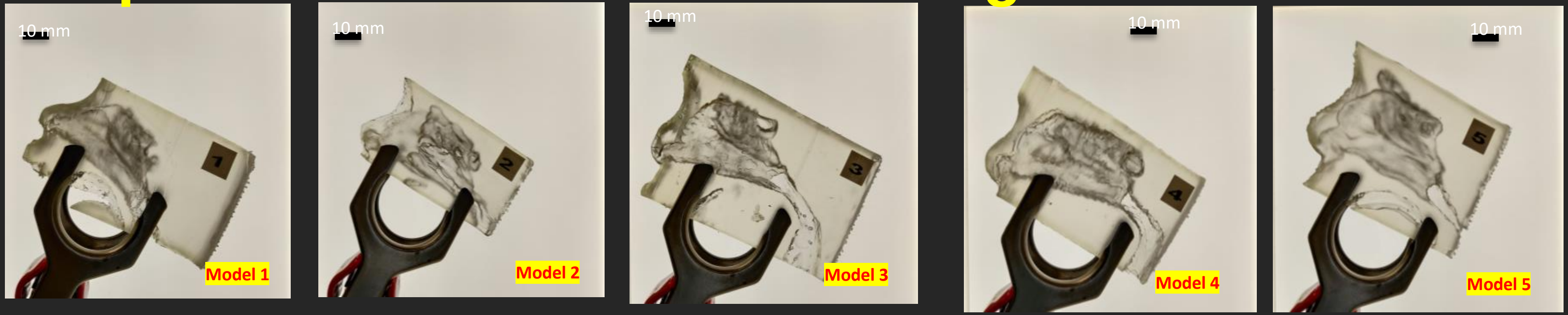

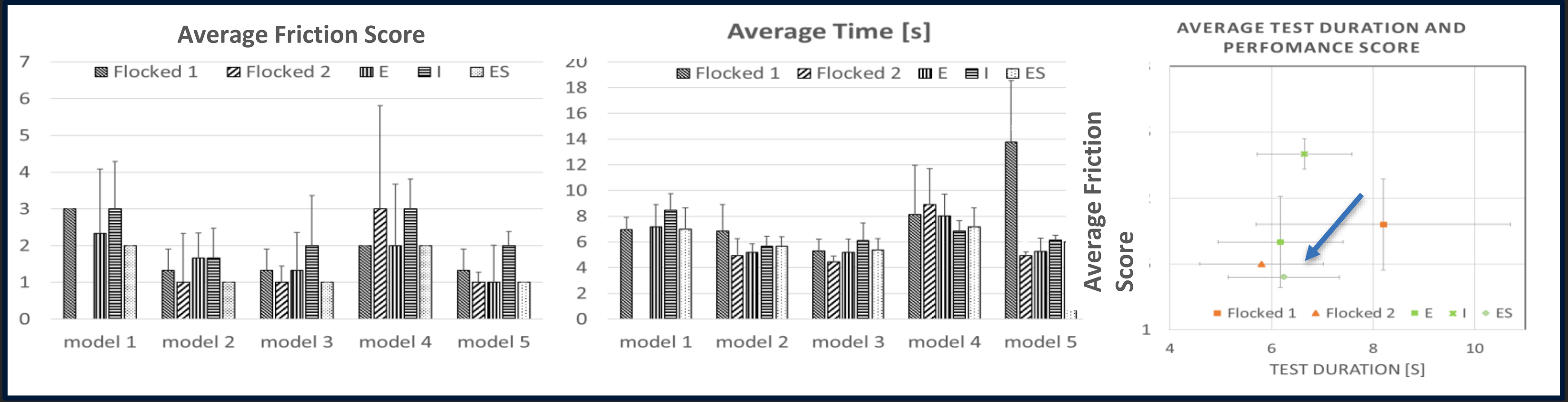

Fig. Testing results comparison based on three repetition of testing swab's procedure on the five anatomical models. Flocked 1 swab was not able to complete the procedure due to very narrow nasal passages of Model 1 A) Average performance score (the lower value the performance is better). B) Average time of procedure in seconds. *Flocked 2* swab was not able to complete the testing procedure due to very narrow nasal passages of Model 1. C) Chart showing relation of time and performance tests results for each of tested swabs.

Manufacturing pipeline

Printing

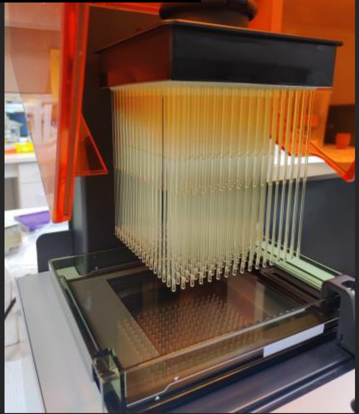

Washing

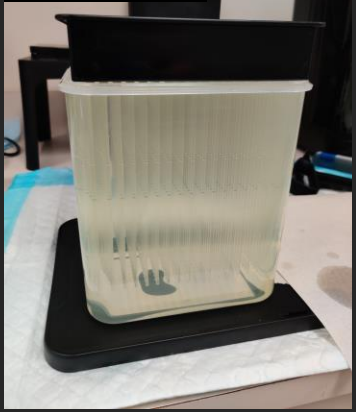

Drying

UV Curing

Packing

Autoclave

Storying

Tensile Testing

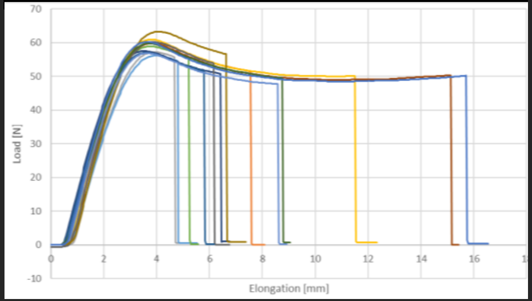

50.000 swabs delivered to clinic

Bioprinting

Multimodal imaging compatible micro-physiological system

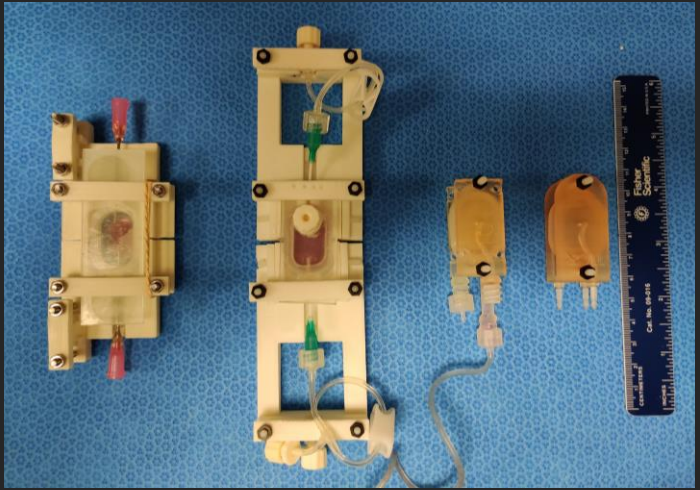

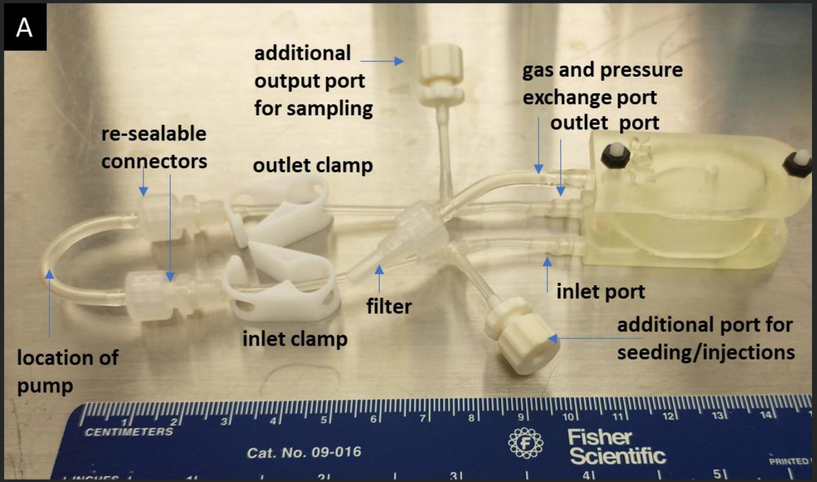

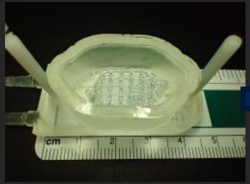

3D Print vascular structure

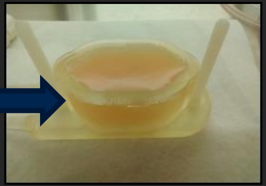

Cast gel + cells surrounding the printed structure

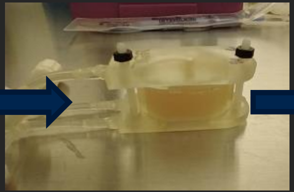

Assemble enclosure, Crosslink gel @ 37 ° C, Evacuate Pluronic @ 4 ° C

Multiple chips perfusing @ 37° C, in a CO_2 incubator

P. Admane at al. Bioprinting, Volume 29, 2023, e00249, https://doi.org/10.1016/j.bprint.2022.e00249

Texas Children's®

BCM Baylor College of Medicine

Compatibility with MR/CT/US

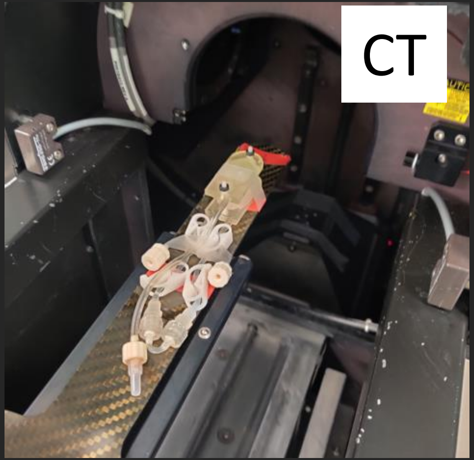

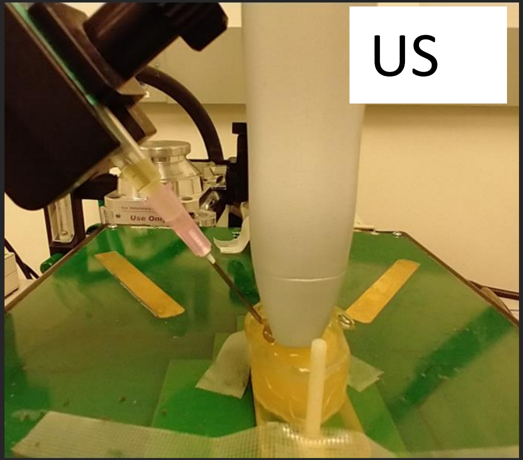

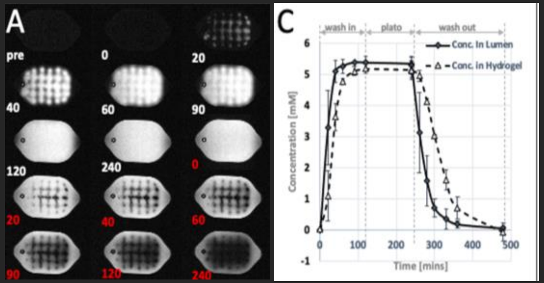

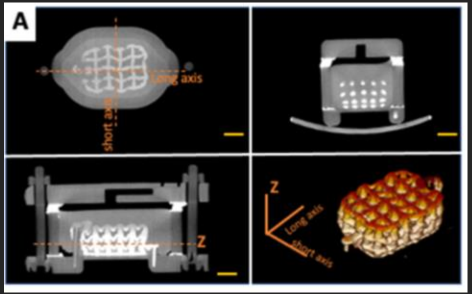

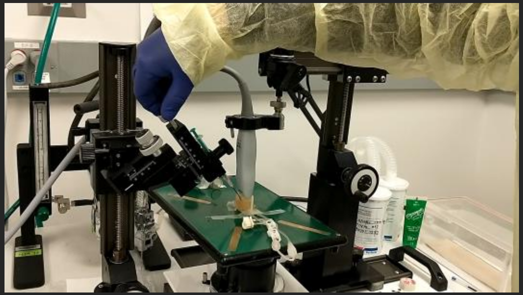

Ultrasound-guided biopsy

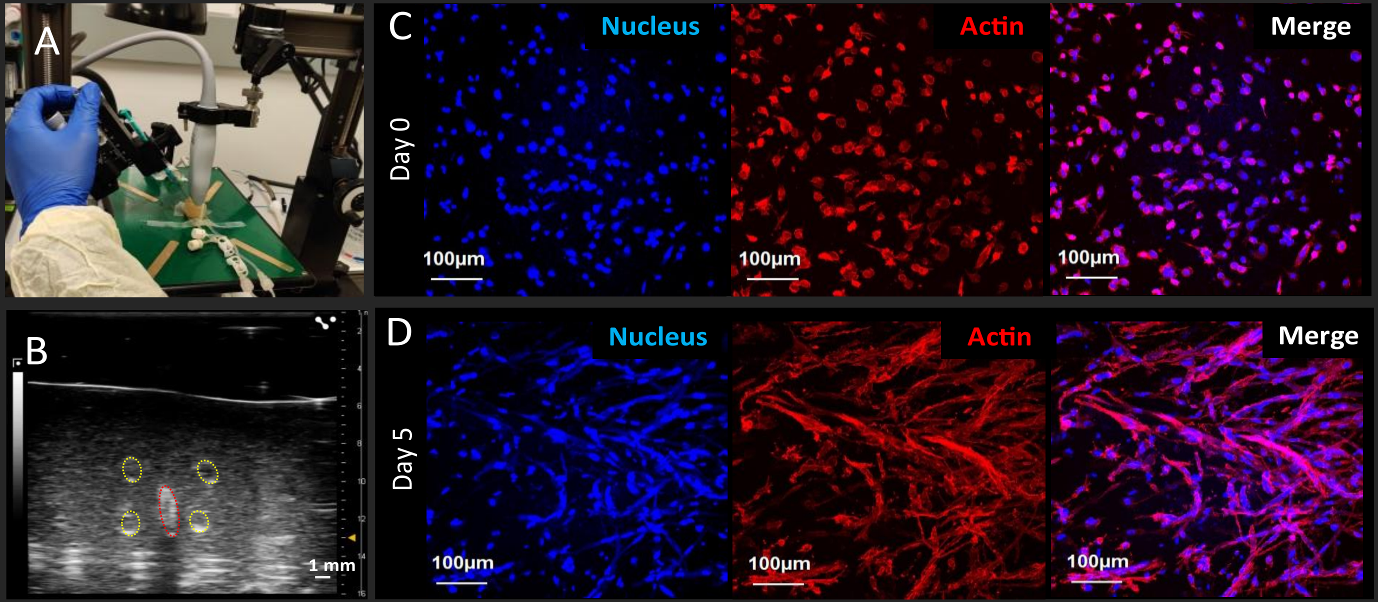

Fig. Ultrasound-guided biopsy of fibroblast-laden perfused MicMPS. *A) Setup of imaging stage with ultrasound probe and injector on top of MicMPS. Biopsy was performed using a 1mL syringe mounted for aspiration of the samples. B) Ultrasound image of a sagittal central plane of the MicMPS. Yellow contours in the image are horizontal channels of printed 3D perfusion grid. Red contour in the center indicates position of the needle for sample collection. C) Microscopy images of biopsy sample of MicMPS tissue on day 0 showing separate channels to demonstrate cell density and cellular morphology (nucleus stain using DAPI, intermediate filament actin stain and merged image). D) Microscopy images of biopsy on day 5.*

Texas Children's®

BCM
Baylor College of Medicine

Ultrasound-guided biopsy

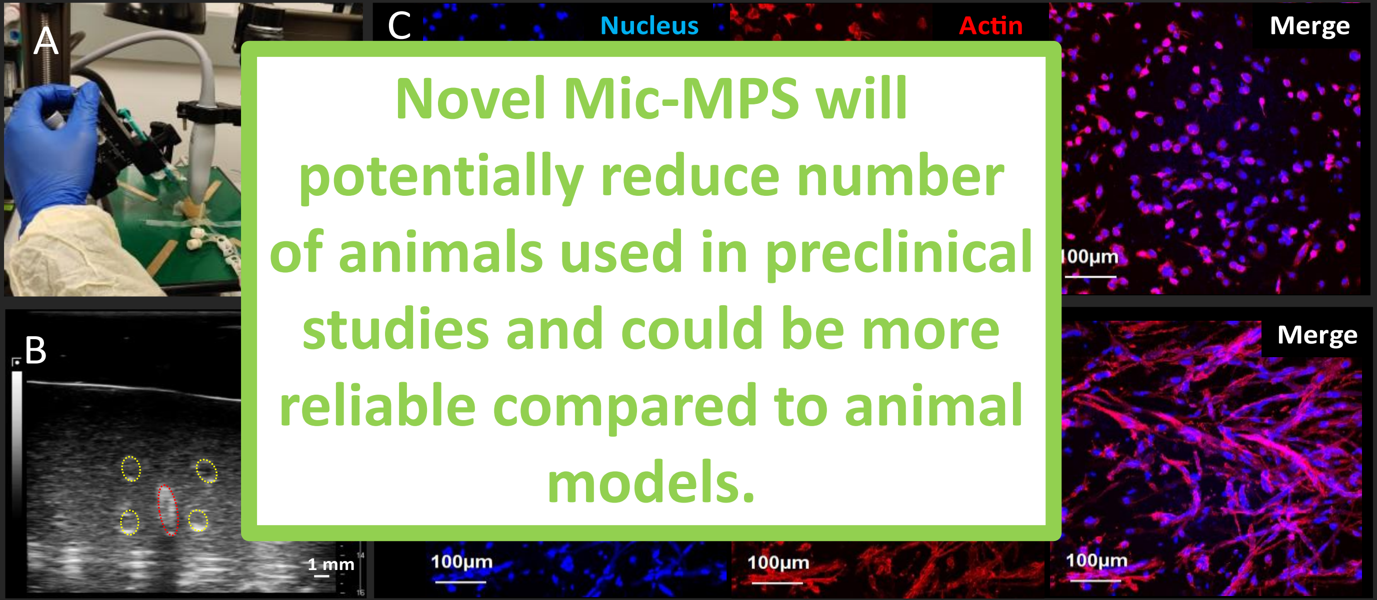

Novel Mic-MPS will potentially reduce number of animals used in preclinical studies and could be more reliable compared to animal models.

Fig. Ultrasound-guided biopsy of fibroblast-laden perfused MicMPS. *A) Setup of imaging stage with ultrasound probe and injector on top of MicMPS. Biopsy was performed using a 1mL syringe mounted for aspiration of the samples. B) Ultrasound image of a sagittal central plane of the MicMPS. Yellow contours in the image are horizontal channels of printed 3D perfusion grid. Red contour in the center indicates position of the needle for sample collection. C) Microscopy images of biopsy sample of MicMPS tissue on day 0 showing separate channels to demonstrate cell density and cellular morphology (nucleus stain using DAPI, intermediate filament actin stain and merged image). D) Microscopy images of biopsy on day 5.*

ML and Radiomics research

Radiomics

- Quantitative approach to data mining of medical images
- Extracts high-dimensional data from standard images to define a novel set of quantifiable imaging patterns or imaging biomarkers
- Proven to be predictive and prognostic regarding clinical outcomes and treatment pathways
- Example

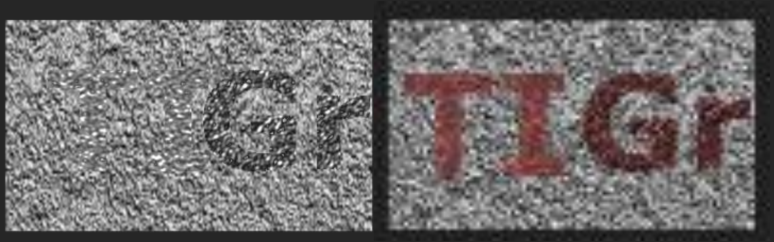

Radiomics Features Classes

(1) Original radiomics features

shape and size descriptors

first-order statistics

texture classes

- gray-level co-occurrence matrix (GLCM)
- gray level run length matrix (GLRLM)
- gray level size zone matrix (GLSZM)
- gray level dependence matrix (GLDM)
- neighboring gray-tone difference matrix (NGTDM)

(2) Logarithmic enhancement of original radiomics features

(3) Wavelet representations of original radiomic features

In research literature 70 up-to 3600 RF are being investigated

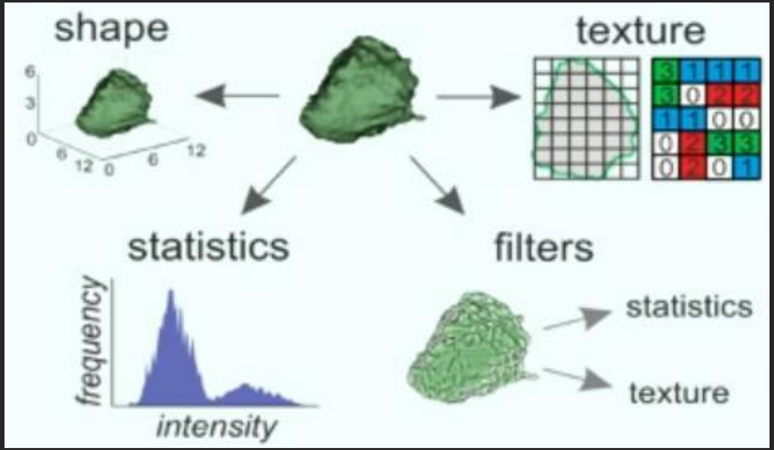

IBSI
image biomarker standardisation initiative

Zwanenburg et al. Radiology. 2020;295(2):328-338

Aerts HJ et al. Jama Oncology 2016

Nano-Radiomic analysis of tumor microenvironment (TME) using nanoparticle contrast-enhanced imaging data

Nano-Radiomics - Radiomic analysis of nanoparticle contrast-enhanced images

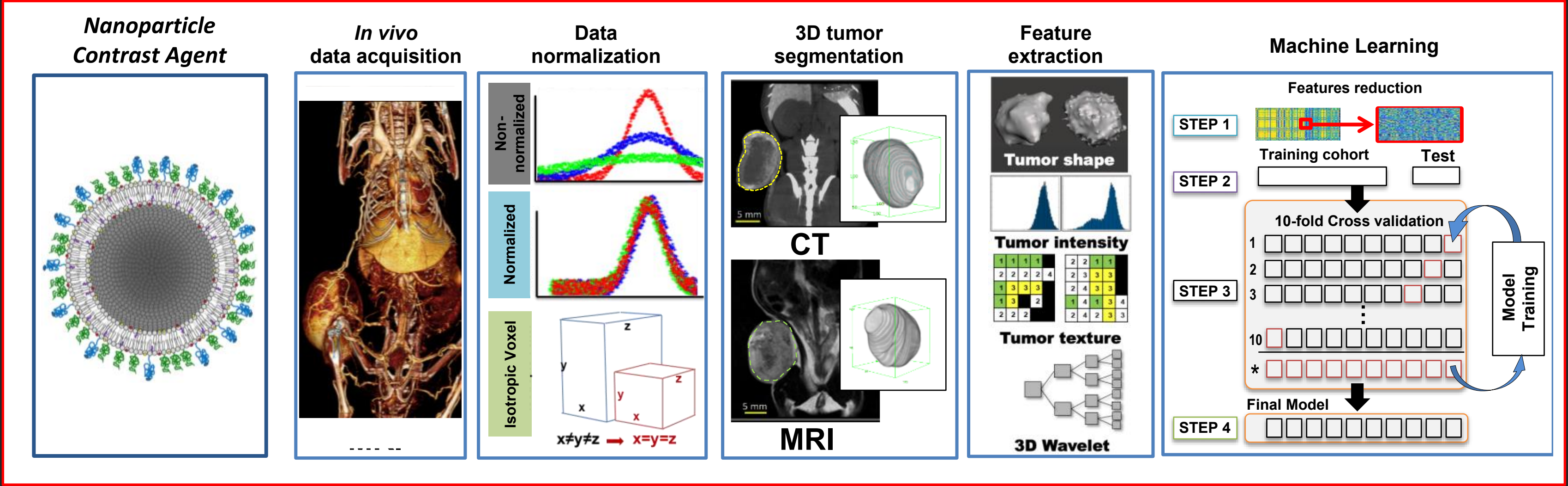

Aerts et al. Jama Oncology (2016)

Microenvironment in Solid Tumors

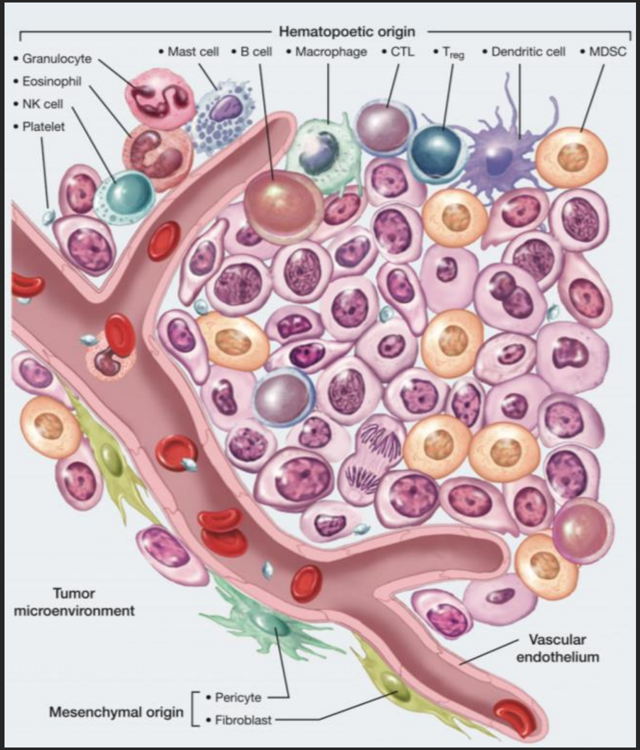

Tumor microenvironment (TME) is immunosuppressive

- Disease progression
- Disease relapse

Monitoring response to TME-directed therapies

- Biopsy: Limited effectiveness due to inter-& intra-tumoral heterogeneity
- Conventional Imaging: Delayed and often variable response
  - Indirect effect on tumor cells
  - Tumor immune cells <<< tumor cells

Investigate nano-radiomics for

- Tumor immune profiling
- Monitoring tumor response to TME-directed cellular immunotherapy

Stratifying Tumors Based on TAM burden Using Nano-Radiomics

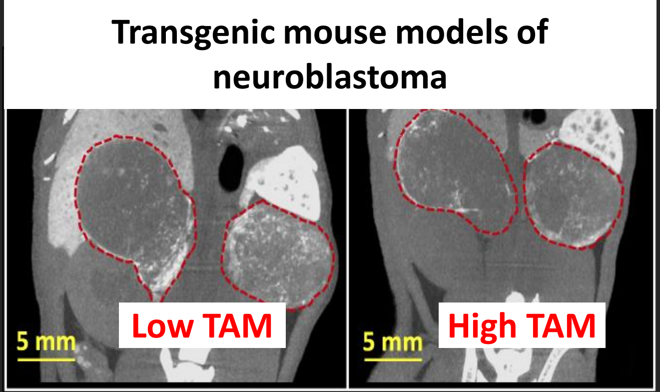

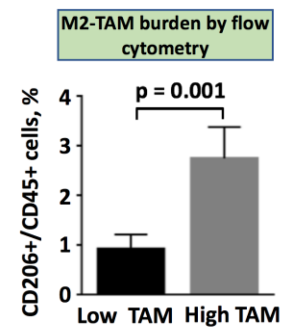

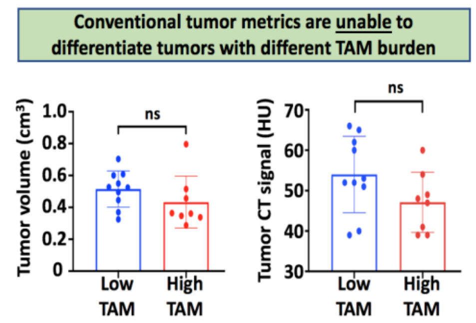

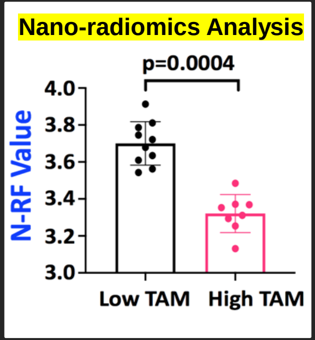

Transgenic mouse models of neuroblastoma with low ($N = 11$) and high ($N = 10$) tumor-associated macrophage (TAM) burden

A Nanoradiomics Approach for Differentiation of Tumors Based on Tumor-Associated Macrophage Burden by Starosolski et al. Contrast Media & Molecular Imaging, 2021

Nano-Radiomics: Early Detection of Aortic Degradation in Mouse Model

Arteriosclerosis, Thrombosis, and Vascular Biology
Volume 41, Issue 4, April 2021; Pages 1534-1548
https://doi.org/10.1161/ATVBAHA.120.315210

American Heart Association.

TRANSLATIONAL SCIENCES

Early Detection of Aortic Degeneration in a Mouse Model of Sporadic Aortic Aneurysm and Dissection Using Nanoparticle Contrast-Enhanced Computed Tomography

Ketan B. Ghaghada, Pingping Ren, Laxman Devkota, Zbigniew Starosolski, Chen Zhang, Deborah Vela, Igor V. Stupin, Eric A. Tanifum, Ananth V. Annapragada, Ying H. Shen, and Scott A. LeMaire

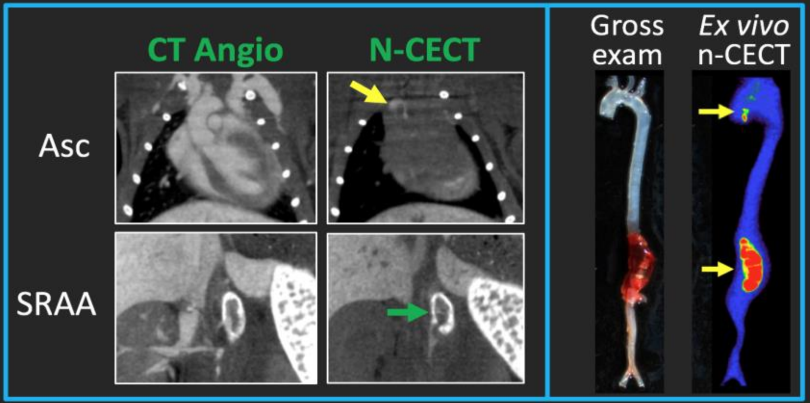

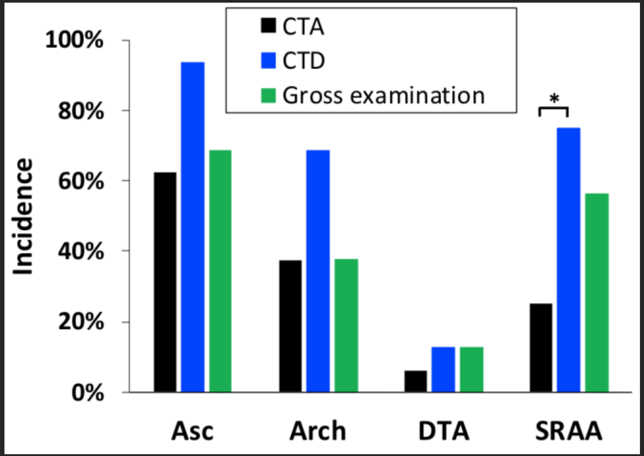

Radiomics

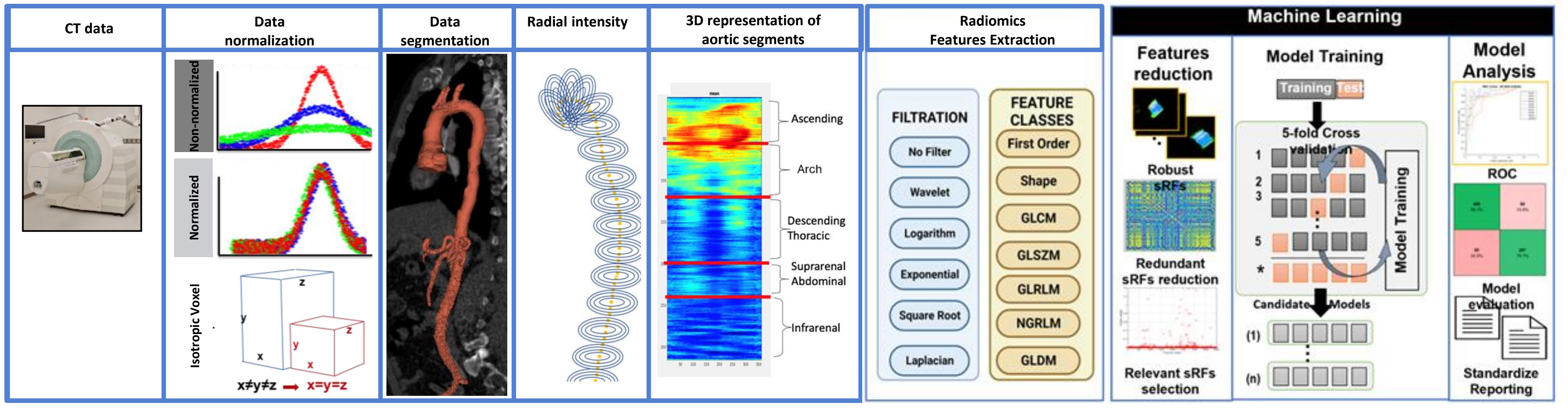

Animals:

Survivors: n=23

Non- survivors: n=8

ML models:

2 RF:
Linear Discriminator
ACC = 74.2%, AUC .79

3 RF:
Linear Discriminator
ACC = 87.1%, AUC .87

5 RF:
Logistic Regression
ACC = 93.5%, AUC .97

(1) Orig. glszm Large Area Hight Gray Level Emphasis
(2) Orig. gldm Dependence Non Uniformity
(3) Wavelet LHL first order Kurtosis
(4) Log sigma 5.0 3D glszm Low Gray Level Zone Emphasis
(5) Log sigma 3.0 3D gldm Dependence Non Uniformity

Clinical Diagnostics

Chest X-rays

Data:

- 1361 chest radiographs
- age: 11.6±9.5 yrs.
- 80.6% < 18 yrs.
- expert annotation :
- (1) positive vs (2) normal vs (3) hardware

Processing:

- Sliding window 3x3cm
- ~300k images
- Radiomics analysis
- Feature selection method
- Classifiers: LR, RF, XGBoost.

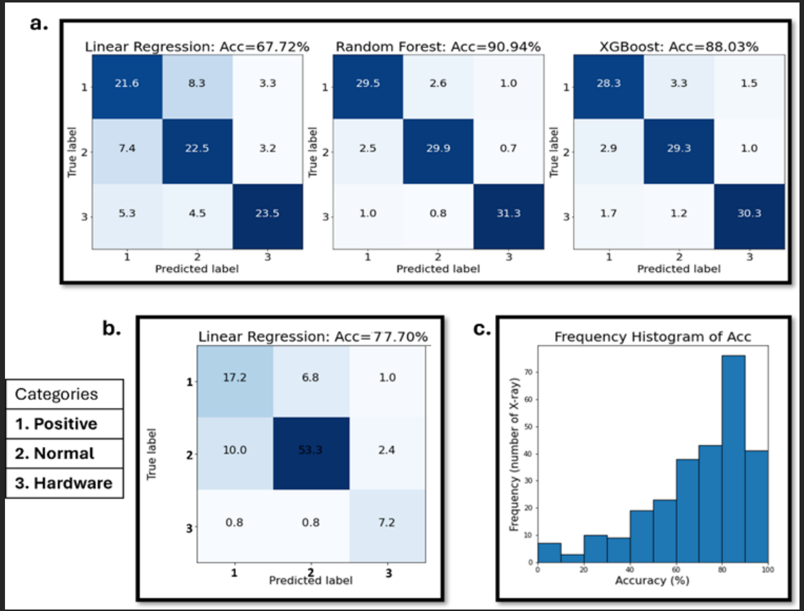

Fig. Classifier performance (a) Validation confusion matrix for Linear Regression, Random Forest and XGBoost model, (b) Testing confusion matrix for Linear Regression, and (c) histogram for individual radiograph patch accuracies.

Md Moin Uddin Atique, Yan Ding, Saad Jafri, Marla Sammer, Ananth Annapragada, Zbigniew Starosolski

Chest X-rays

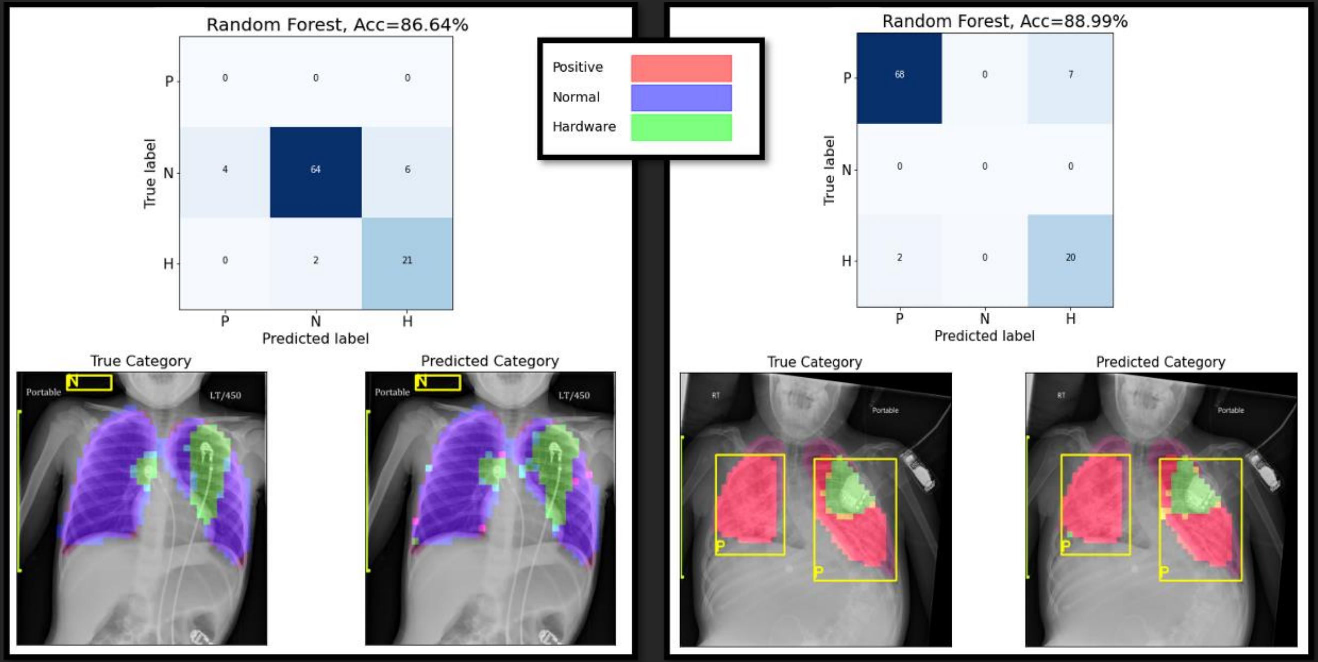

Fig. Confusion matrix (top) and color marked true category (left bottom) and predicted category (right bottom) for two example subjects. The color for corresponding categories is shown in the legend.

Clinical Prognostication

AI tool for risk analytics: Not Accidental Trauma (NAT)

- False Negative AND False Positive
- 2016- 7.4 million children referred 676,000 deemed victims (1,750 fatalities)
- ~25% victims <3yrs (70% of fatalities)

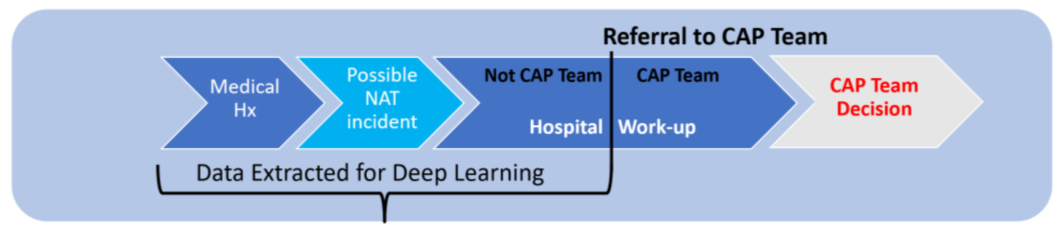

Fig. The records were processed to extract only those notes written before the first note from a Child Abuse Pediatrics team

(Source: Child Maltreatment 2016, US Depth. Of HHS)

Akshaya V. Annapragada, Marcella M. Donaruma-Kwoh, Ananth V. Annapragada, Zbigniew A. Starosolski
https://doi.org/10.1371/journal.pone.0247404

EHR – Free text - example

Neurosurgery Consult Note Date: 04/19/22 Time: 1:32 AM Patient Name: NAME NAME Date of Admission:

History

76543210 Attending Physician: DOB PCP: Sanchez-Burgos, Teodoro Y, MD Sex: female Unit: Age: 5 m.o. Room: eason for Consult Skull fracture HPI NAME NAME is a 1 m.o. female who presents with a skull fracture after an acute head trauma 10 d ago (4/12) when he fell from an hammock. The kid hit head, immediately cried. He is otherwise healthy. Taken to HospitalOSH ER, got head CT that showed nondisplaced skull fx. Returned to baseline, had emesis x 1, and the patient was discharge home with PCP follow up. PCP referred to neurology who say the patient on 1/11 with instructions to bring head CT film CD. Parents brought head CT the following day for review. Neurology concerned for NAT, instructed mother to bring pt back to the ER. Mother reports normal behavior/activity, PO intake and UOP/stool habits. Denies fever, lethargy, AMS, sz activity, fussiness, decreased PO, decreased UOP, bruising, bleeding. PMH/Developmental History Past Medical History Diagnosis Date ? Skull fracture ? IUGR (intrauterine growth restriction) Review of Systems None Allergies Allergies Allergen Reactions ? No Known Drug Allergy ? .Food No Known Food Allergy Medications Active Scheduled Medications: Active PRN M

Labs/Exam

story Family History Problem Relation Age of Onset ? Neurologic disease Neg Hx Social History Other T le Social History Narrative Lives with parents. She is only child. Mother is teacher assistant. Father is quality control for oil rig parts. Physical Examination Patient Vitals for the past 24 hrs: BP Temp Temp src Pulse Resp SpO2 Weight 04/19/22 1400 90/63 mmHg 97.6 ?F (36.4 ?C) Axillary 142 34 - - 04/19/22 0922 80/52 mmHg 98.1 ?F (36.7 ?C) Axillary 146 36 100 % - 04/19/22 1012 (!) 101/87 mmHg - - - - - - 04/19/22 0750 (!) 74/63 mmHg - - 150 38 - - 04/19/22 0240 - - - 147 - - - 04/19/22 0849 - 99 ?F (37.2 ?C) Axillary - 36 - 6.98 kg (15 lb 6.2 oz) Neurologic Exam Mental Status: Cranial Nerves: CN II ? pupils equal, round and reactive to light, blinks to bright light bilaterally CN III/IV/VI ? vestibulo-ocular reflexes intact to cardinal directions of gaze CN V ? rooting reflex intact CN VII ? facial symmetry during crying CN VIII ? responds to sound CN IX/X/XII ? normal sucking, intact gag CN XI ? sternocleidomastoid movement noted Motor: Normal truncal and appendicular tone. Spontaneously moves all extremities against gravity. Reflexes: Symmetrical reflexes at knee, ankle, biceps Sensation: Responds to touch in all 4 limbs Si

Imaging Report

s 04/19/22 0125 AST 35 ALT 13 Recent Labs 04/19/22 1112 WBC 4.95* HGB 10.3 HCT 30.5 PL 494* SEG 4.9 BAND 3.3 LYMP 55.9 MONOS 4.2 EOS 0.8 BASO 0.8 Recent Labs 04/19/22 1011 PROTIM 14.4 PTT 40.7* INR 1.1 Significant Imaging CT head shows left parietal skull fracture with small subdurals. Assessment Diagnosis: Left parietal skull fracture with small frontal subdurals bilaterally. Plan Non neurosurgical intervention at this point. PT admitted by trauma for a NAT work up. Follow up in head trauma clinic in 4 weeks. Please call Neurosurgery Office (No. 10 Digits)

Texas Children's®

BCM Baylor College of Medicine

Schematic of Patient Record Selection and Processing

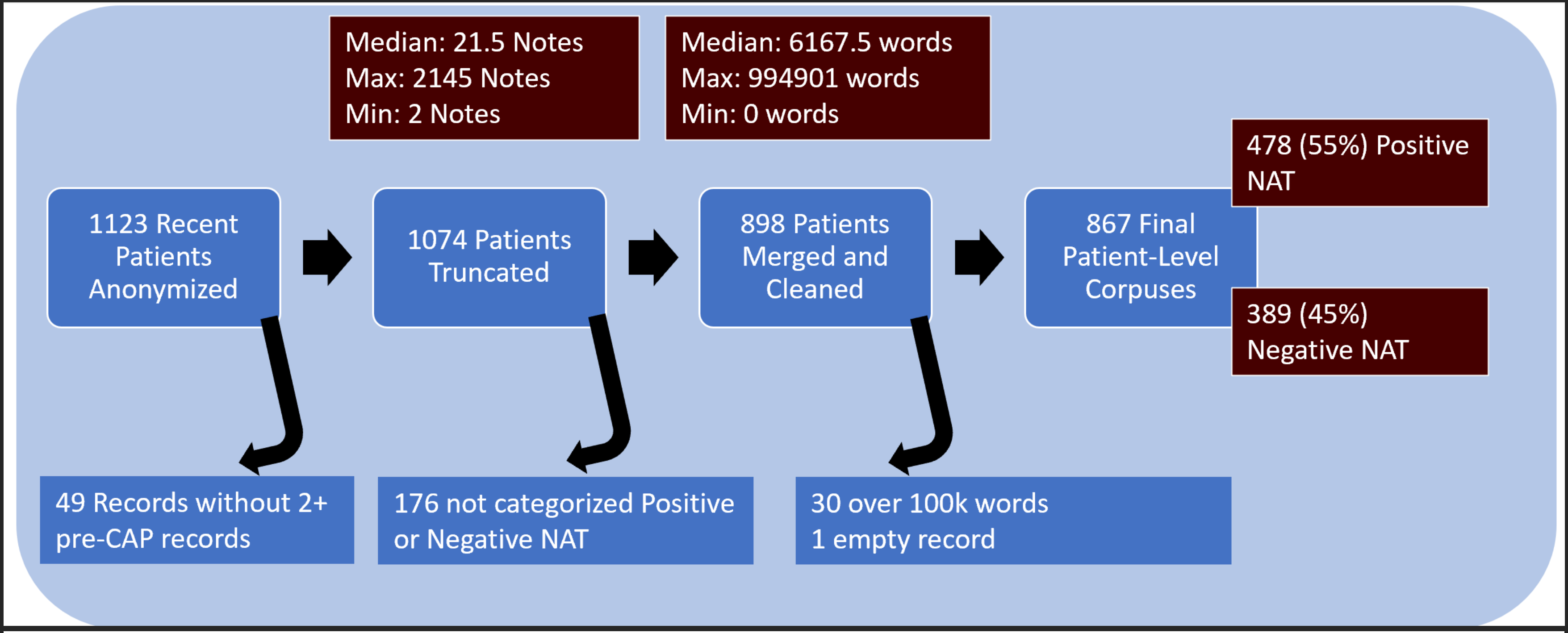

Fig. Schematic of Patient Record Selection and Processing all available records for patients worked-up for suspected not accidental trauma between 2015 and 2019

Pipeline for the NAT classification

Notes
Free text

Pre-processing

Embedding layer
- GLOVE
- MIMIC-III
- **WE-PED**

Neural Net
- MPR
- CNN

Classifier

Model	Accuracy	ROC-AUC
WE-GLOVE	65.8 ± 2.8%	68.3±3.5%
WE-MIMIC-III	66.4 ±3.8%	64.5±7.5%
WE-PED	**92.0 ± 3.0%**	**96 ± 1.0%**
BOW	89.9 ± 2.6%	93.1 ± 2.2%
Rule-Based	76.6 ± 3.7%	81.4 ± 5.2%

Pipeline for the NAT classification

Notes
Free text → Pre-processing → Embedding layer
- GLOVE
- MIMIC-III
- **WE-PED**

→ Neural Net
- MPR
- CNN

→ Classifier

Model	Accuracy	ROC-AUC
WE-GLOVE	65.8 ± 2.8%	68.3±3.5%
WE-MIMIC-III	66.4 ±3.8%	64.5±7.5%
WE-PED	**92.0 ± 3.0%**	**96 ± 1.0%**
BOW	89.9 ± 2.6%	93.1 ± 2.2%
Rule-Based	76.6 ± 3.7%	81.4 ± 5.2%

Pipeline for the NAT classification

Notes
Free text → Pre-processing → Embedding layer
- GLOVE
- MIMIC-III

→ Neural Net
- MPR
- CNN

→ Classifier

Model	ROC-AUC
WE-GLOVI	68.3±3.5%
WE-MIMIC-	64.5±7.5%
WE-PED	**96 ± 1.0%**
BOW	93.1 ± 2.2%
Rule-Basec	81.4 ± 5.2%

AI-risk analytics could help predict NAT based on EHR and give indications for acute preventive care, especially in facilities without a CAP team in place.

THANK YOU

Feedback/Questions:

Zbigniew Starosolski
zastaros@texaschildrens.org

Texas Children's Hospital®

Baylor College of Medicine

TIGr: Translational Imaging Group